Available online at www.sciencedirect.com
SCIENCE DIRECT®
Journal of Crystal Growth 268 (2004) 242–248
JOURNAL OF CRYSTAL GROWTH
www.elsevier.com/locate/jcrysgro

Low-temperature solution approach toward highly aligned ZnO nanotip arrays

Chin-Hsien Hung*, Wha-Tzong Whang

Department of Materials Science and Engineering, National Chiao Tung University, 1001 Ta Hsueh Road, Hsinchu 30049, Taiwan

Received 3 March 2004; accepted 3 May 2004

Communicated by M. Schieber

Abstract

Highly aligned and free-standing ZnO nanotip arrays grown on the ZnO films by soft chemical method are proposed. X-ray diffraction analysis shows that the ZnO nanotips are hexagonal wurtzite structure, and the *c*-axes of nanotips are perfectly along the substrate surface normal. HRTEM demonstrates the ZnO nanotip to be a single crystal. Room temperature photoluminescence of the ZnO nanotips has a strong UV emission band at 378 nm. The field emission of ZnO nanotip arrays shows a turn-on field of about 10.8 V/μm at a current density of 0.1 μA/cm and emission current density up to about 1 mA/cm^2 at a bias field of 19.5 V/μm. The mild technique for fabricating ZnO nanotip arrays is believed to open novel possibilities for nanoscale optoelectronic device applications.

PACS: 81.10.Dn; 78.55.Et

Keywords: A1. Low dimensional structures; A2. Growth from solutions; B1. ZnO

1. Introduction

Owing to the unique geometries of small radii of curvature, the nanotips have attracted significant interests for the potential applications such as the probing tip for the high-resolution imaging atomic force microscopy [1], the photonic crystal for waveguide and the field emitter for flat-plane displays [2]. For the field emitter arrays technologies, the manipulation of high density, vertical aligned and well-ordered fine tips are particularly desirable. Currently, developing high-performance field emitter mainly relies on materials with low work function and thermal stability under the high vacuum environment, such as carbon-based (carbon nanotubes, diamond-like carbon) [3], silicon-based (Si, SiN, SiCN) [4], oxide-based (MoO_2, MoO_3, ZnO) [5,6], and other semiconductor materials [7]. Among these materials, zinc oxide (ZnO) is a wide band-gap (3.4 eV) and large exciton binding energy (60 meV) semiconductor

*Corresponding author. Tel.: +886-35-731873; fax: 886-35-724727.

E-mail addresses: jim.mse89g@nctu.edu.tw (C.-H. Hung), wtwhang@mail.nctu.edu.tw (W.-T. Whang).

0022-0248/$ - see front matter © 2004 Elsevier B.V. All rights reserved.
doi:10.1016/j.jcrysgro.2004.05.009

compound, which is useful for light emitting diodes, room-temperature nanolasers, gas sensors, piezoelectric devices, and solar cells [8], etc. Recently, one-dimensional (1D) ZnO nanostrustures, such as nanowires, nanotubes and nanorods, have attracted great attentions due to the excellent physical and chemical properties that are highly different from the bulk materials.

Generally, 1D ZnO nanostructures are synthesized by the following methods: anodic alumina template [9], metal catalyst-assisted vapor phase transport (MCVPT) [10], metal-organic chemical vapor deposition (MOCVD) [11], metal-organic vapor epitaxy (MOVPE) [12] and common thermal evaporation method [13]. Much efforts have been devoted to obtain highly aligned and well-separated (i.e. isolated standing) 1D ZnO arrays, which are crucial for developing the next generation of nanoscale electronic and optoelectronic devices. Such perfectly aligned ZnO nanowire arrays are achieved via MCVPT or MOVPE techniques [8,10,14]. Huang et al. demonstrated the aligned ZnO nanowire arrays epitaxially grown on (0 0 0 1) sapphire substrate by using MCVPT technique with the gold catalyst at 900–925°C [8]. However, the necessary of relative high temperature and expensive sapphire substrates restrict the production and wide applications of 1D ZnO arrays. In addition, the MCVPT technique is not suitable for growing sharply tips since the metal catalyst droplets would form at the terminating growth front. Notably, the soft chemical route greatly facilitates the approach to scaled-up fabricated 1D ZnO nanostructures with relative low-cost, which also has been demonstrated to be very efficient in synthesizing single crystal structure at a remarkably low temperature [15]. Vayssieres et al. reported the aligned ZnO microsize rod arrays growing on conducting tin oxide glass by hydrothermal procedure at 95°C aqueous solution [16]. Liu et al. utilized the well-defined (0 0 1) facet microrods as the substrates to grow helical structures of ZnO nanorod and column arrays [17]. Recently, we proposed the using of a layer of nanoparticles with self-seeding assistance to attain ZnO nanorods on ITO substrate [18]. However, the polycrystalline nano-seeds on the substrate generated the random orientations of our nanorods, so the nanorod alignment was unsatisfied. To data, fabricating perfectly aligned and well-isolated 1D ZnO nanoarrays on the Si substrates with soft chemical method is a valuable challenge, which would benefit in the electronic device integrations due to the mild growth conditions. To our knowledge, growing well-aligned ZnO nanotip (nanoneedle) arrays on Si substrate rarely succeeded except using the MOCVD-based method at temperature 400–500°C [19,20]. In this study, we grew vertical and isolated single-crystal ZnO nanotip arrays on a ZnO thin film by soft chemical technique at a low temperature of 95°C without any metal catalyst or template. The field emission (FE) of our ZnO nanotip arrays shows a turn-on field of 10.8 V/μm at a current density of 0.1 μA/cm. Moreover, we also successfully fabricated the self-oriented nanotip arrays on ZnO microrod by soft chemical route. This fascinating morphology suggested that our new strategy might provide an insight for building a controllable well-ordered multiple nanostructures at a significant low temperature.

2. Experimental procedure

All the chemicals from Tokyo Chemical Industry were used as received without further purification. ZnO nanotip arrays growth was prepared by the wet chemical technique, as reported by Vayssieres et al. [16]. In this study, 0.1 g of zinc nitrate ($Zn(NO)_3 \cdot 6H_2O$, 3×10^{-3} M) and 0.1 g of methenamine ($C_6H_{12}N_4$, 6×10^{-3} M) were dissolved in 100 ml aqueous solution as the precursor solution. Prior to growing ZnO nanotips, a thin ZnO layer (ca. 200 nm) was deposited on the Si substrate by radio frequency sputtering. The substrate was then put into a bottle filled with precursor aqueous solution in the oven at 95°C for several hours. After the crystal growth, the final products were rinsed with distilled water several times, and then dried in oven at 100°C for 4 h. The morphology of as-synthesis products was further characterized and analyzed by scanning electron microscopy (SEM) (JOEL JSM-6500F at 10 kV) and high-resolution transmission electron microscopy (HR-TEM) (JOEL 2010F at 200 kV).

Photoluminescence spectrum was also measured at room temperature using He-Cd laser with a wavelength 325 nm as excitation source.

3. Result and discussion

The surface morphology of as-grown ZnO nanotip arrays on the ZnO film substrate was studied by the field-emission scanning electron microscope (FE-SEM). Figs. 1a and b show the top and tilted views of low-magnification SEM images. The numerous nanotips appear as bright dots and are well-separated across the entire substrate, implying that a large density of ZnO nanotips preferentially grew normally to the substrate surface, and almost isolated from each other with a density of approximately 1.22×10^{10} tips/cm^2. The higher-magnification image (Fig. 1c) further shows the formation of a regular nanotip arrays with a perfectly vertical alignment. The nanotips are found to grow from the tops of nano-grained film and the spacing between well-oriented nanotips estimates about 100 nm. The detail morphology can be observed by high magnification side-view image, as shown in Fig. 1d. The nanotips are parallel to each other and perpendicular to ZnO thin film. The base diameter of a nanotip is around 70 nm and the length is around 410 nm. The length could be further controlled by changing the growth parameters, such as reaction times. Typically, the length of a nanotip decreases to $\sim$160 nm in 95°C aqueous solution for 2 h growth. In contrast

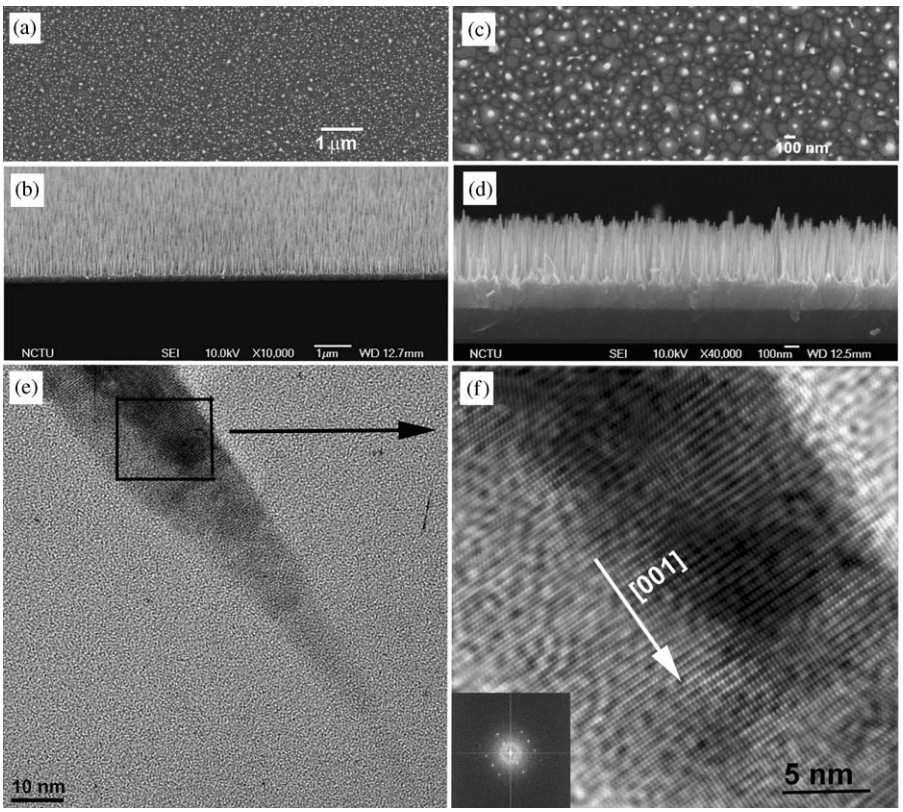

Fig. 1. SEM images show highly aligned ZnO nanotip arrays grown on the ZnO thin film at 95°C aqueous solution for 6 h. Low-magnification images from (a) top view and (b) tilt view reveal that high density of well-oriented ZnO nanotips were dispersively distributed on the substrate. (c) top and (d) side view of high-magnification SEM images. (e) TEM image of a typical ZnO nanotip. (f) high-resolution TEM image taken from the edge of ZnO nanotips and the corresponding fast Fourier-transform pattern (inset).

to the hemispherical end and hexagonal-shaped structure of ZnO nanorod grown by hydrothermal techniques reported previously [16,18,21,22], the feature of ZnO nanotips in this study obviously has a sharp apex and conical morphology. The structural characterization of the ZnO nanotips was investigated by transmission electron microscopy (TEM) and the typical TEM image of an individual nanotip is depicted in Fig. 1e. The nanotip end clearly has an extremely sharp morphology with an apex angle about 13°. The high-resolution TEM image (HRTEM) in Fig. 1f shows a single crystal structure of the ZnO nanotip. The lattice spacing of about 0.26 nm between adjacent lattice planes corresponds to the distance between (0 0 2) crystal planes, meaning that the [0 0 1] direction is a common growth direction of the ZnO nanotip. Energy dispersive X-ray spectroscopy (EDX) analysis shows the nanotips only contain Zn and O, confirming that no other metal impurity exists. The crystal structure of ZnO nanotips was investigated by X-ray diffraction. As shown in Fig. 2, only two diffraction peaks of (0 0 2) and (0 0 4) of wurtzite ZnO were observed, implying that the (0 0 2) planes of ZnO nanotips were perfectly oriented perpendicularly to the surface.

Photoluminescence spectrum (PL) of ZnO nanotip arrays was measured at room temperature using a He-Cd laser with an excitation wavelength of 325 nm. The PL spectrum in Fig. 3 exhibits a strong UV emission at 378 nm (3.29 eV), agreeing

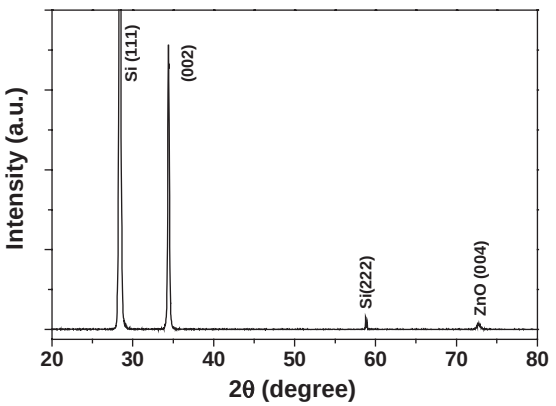

Fig. 2. X-ray diffraction pattern of ZnO nanotip arrays grown on the ZnO film.

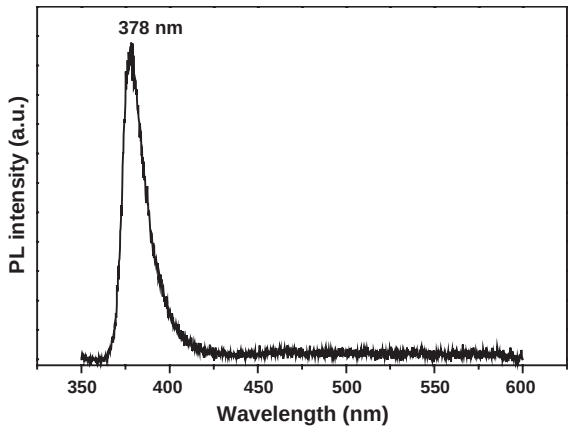

Fig. 3. PL spectrum of ZnO nanotip arrays measured at room temperature.

well with the band gap of bulk ZnO (~380 nm) which comes from recombination of free excitons via exciton–exciton collision process [23]. Generally, a green–yellow emission could be observed in the PL spectrum, which comes from the recombination of photogenerated hole with a singly ionized charge state of specific defect [24]. However, the green–yellow emission did not appear in our sample. Therefore, the results of PL spectrum show that our low-temperature growth method can produce a low concentration of oxygen defects and high optical quality of singe crystal ZnO nanotips.

The growth mechanism of ZnO nanotip arrays on a substrate described here could be based on conventional crystal growth model of solution chemistry [16]. Accordingly, the crystal nucleation and growth in the solutions are controlled by interface free energy. In present work, the column-like (0 0 2) ZnO thin film was deposited on the Si substrate as a self-seeding and buffer layer prior to the crystal growth. Note that no ZnO nanotip was formed on the bare Si substrate under the same growth conditions. Certainly, the ZnO film in our work can effectively provide nuclei sites and reduce interface energy barrier for ZnO crystal growth. Upon the hydrolysis-condensation reaction, the reactant [$Zn(OH)^+$] diffused onto the ZnO film surface and gradually formed a saturating situation between ZnO film/solution interface. As soon as reaching a critical saturation point, the

nuclei of ZnO crystals simultaneously occurred on the column-like (0 0 2) ZnO film, then the ZnO crystals began to precipitate and resulted in a preferential orientation along ZnO [0 0 1] by direct homoepitaxial growth. The nano-grained {0 0 2} ZnO film provided perfectly well-separated and oriented nuclei for ZnO crystals growth, producing a well-ordered and vertically aligned nanotip arrays on the substrate. Moreover, the concentration gradient of reactant created a driving force for further crystal growth. According to "the lowest energy" argument on polar crystal growth by Laudise's et al. [25], the growth velocity along $\langle 0\,0\,1 \rangle$ direction could be much higher than that along $\langle 1\,0\,1 \rangle$ and $\langle 1\,0\,0 \rangle$ directions. In fact, it is well-known fact that the crystal facets with a faster growth velocity are easier to disappear and eventually result in the appearance of the crystal only built up by slower growth rate facets. Recently, Park and co-workers [19] also proposed that sharp-tipped ZnO nanoneedle formation could originate from a higher growth rate along the *c*-axis direction than that along the in-plane direction. We therefore conclude that the tips-like ZnO geometry mainly resulted from higher growth rate along $\langle 0\,0\,1 \rangle$ direction.

We found that the nanotip arrays can also be grown on ZnO microrods by similar low-temperature technique which formed a "nanotips-rod" geometry. Prior to achieving desired nanostructures, the microsize ZnO rods were deposited onto ITO substrate by equimolar (0.1 M) of zinc nitrate and methenamine aqueous solution at 90°C for 24 h. When the (0 0 1) facets of microrods served as nuclei sites, the ZnO nanotip arrays dispersively self-oriented along the well-defined hexagonal facet (0 0 1) plane with a density of about 200 tips/rod, as shown in Fig. 4a. Comparing with the previous report of growing 1D ZnO on microrod-based substrates [17] which formed a much lower density (<20 nanorods/rod) of helical-like ZnO nanorods, our method should base on

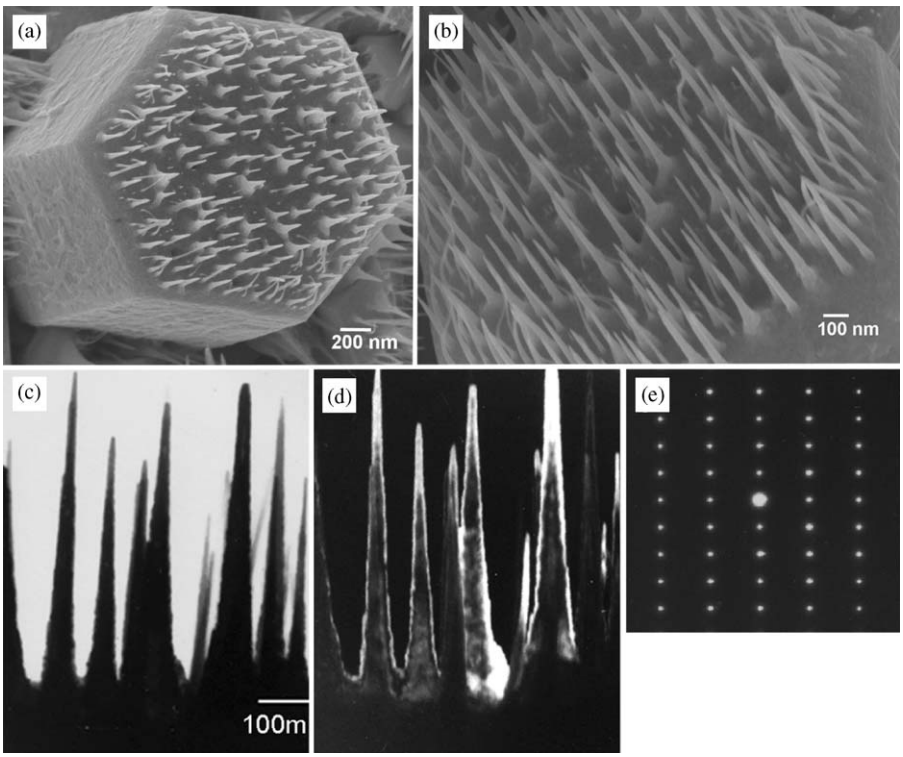

Fig. 4. (a,b) SEM images show the as-grown ZnO nanotip arrays self-organized on the ZnO rod. (c) bright-field and (d) dark-field TEM images from the nanotips-microrod junction region and (e) the corresponding diffraction pattern of microrod.

different growth mechanism. Fig. 4b is a higher-magnification SEM image taken from the top of a microrod. Obviously, the ZnO nanotips are precisely grown perpendicular to the (0 0 1) surface of the microrod, where these nanotips show a conical shaped cross-section and around 250 nm in length, with the base diameter of 60 nm and tip diameter less than 15 nm. The typical bright-field, dark-field images and the corresponding electron diffraction pattern of the ZnO nanostructures captured in side-view are also depicted in Figs. 4c–e, respectively. The results indicate that the homoepitaxial orientation growth of the nanotip arrays only occurred on the hexagonal basal plane of the microrod.

The field emission measurement of ZnO nanotip arrays was carried out in a vacuum under a pressure of $\sim 10^{-6}$ Torr at room temperature. A cylinder electrode of 2.2 mm diameter was placed above the nanotips top surface with a distance of 50 μm. Keithley 237 was employed as a power supply and a current meter. Fig. 5a shows the typical result of the field emission current density versus the applied electric field. The turn-on electric field for the ZnO nanotips was about 10.8 V/μm at a current density of 0.1 μA/cm, and the emission current density reached about 1 mA/cm^2 at a bias field of 19.5 V/μm. The field emission current–voltage characteristics can be expressed by Fowler–Nordheim (F–N) theory:

$$J = (AE^2\beta^2/\Phi)\exp(-B\Phi^{3/2}/\beta E),$$

where J is the emission current density (A/cm^2), E is the applied field (V/cm), β is the field enhancement factor related to the emitter geometry, Φ is the work function of the emitter, A and B are the constants with values of 1.56×10^{-10} (A/V^2 eV) and 6.83×10^9 (V/eV$^{3/2}$ μm), respectively. By plotting $\ln(J/E^2)$ versus $1/E$ in Fig. 5b, two-stages slope behaviors were observed in a measured range. Such characteristics are also perceived in many other types of field emitters [26], which may result from the variation of the tips local field. The β values are derived from fitting the experiment curve to F–N theory by assuming the ZnO nanotips work function of 5.4 eV. Therefore, the field enhancement factor of ZnO nanotip arrays was estimated to be about 590 for β_1 and 270 for β_2. These values are comparable to the reports of needle-like ZnO nanowires [27,28], indicating that the mild method for manufacturing ZnO nanotips arrays would have a great potential in field emitter technologies.

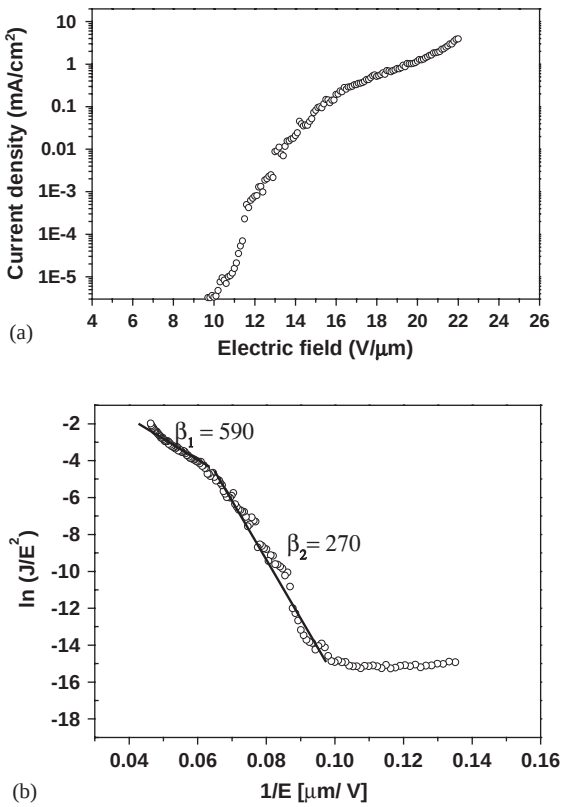

Fig. 5. (a) Field emission current density versus electric field of ZnO nanotip arrays on Si substrate and (b) the corresponding F–N plot.

4. Conclusions

We have successfully produced uniformly well-separated ZnO nanotip arrays which are excellent oriented and vertically aligned on the ZnO film using a soft chemical route under simple and mild conditions. The soft growing method also has been extended to synthesize well-aligned nanotip arrays on ZnO microrods. The field-emission characteristics of ZnO nanotip arrays showed a turn-on field of about 10.8 V/μm at a current density of

0.1 μA/cm. This advanced technique for ZnO nanotip array fabrication is believed to open novel possibilities for nanoscale optoelectronic device applications.

Acknowledgements

The authors would like to thank H. G. Chen for their help in the HRTEM measurement. This research was supported by the National Science Council of the Republic of China under Grant NSC-922216E009013 and Lee and MTI center in NCTU on photonic devices and modules project.

References

[1] A. Rothschild, S.R. Cohen, R. Tenne, Appl. Phys. Lett. 75 (1999) 4025.
[2] V.V. Poborchii, T. Tada, T. Kanayama, Appl. Phys. Lett. 75 (1999) 3276.
[3] J.I. Sohn, S. Lee, Y.H. Song, S.Y. Choi, K.I. Cho, K.S. Nam, Appl. Phys. Lett. 78 (2001) 901.
[4] H.C. Lo, D. Das, J.S. Hwang, C.H. Hsu, C.F. Chen, L.C. Chen, K.H. Chen, Appl. Phys. Lett. 83 (2003) 1420.
[5] C.J. Lee, T.J. Lee, S.C. Lyu, Y. Zhang, H. Ruh, H.J. Lee, Appl. Phys. Lett. 81 (2002) 3648.
[6] J. Zhou, N.-S. Xu, S.-Z. Deng, J. Chen, J.-C. She, Z.-L. Wang, Adv. Mater. 15 (2003) 1835.
[7] J. Chen, S.Z. Deng, N.S. Xu, S.H. Whang, X.G. Wen, S.H. Yang, C.L. Yang, J.N. Wang, W.K. Ge, Appl. Phys. Lett. 80 (2002) 3620.
[8] M.H. Huang, S. Mao, H. Feick, H. Yan, Y. Wu, H. Kind, E. Weber, R. Russo, P. Yang, Science 292 (2001) 1897.
[9] M.J. Zheng, L.D. Zhang, G.H. Li, W.Z. Shen, Chem. Phys. Lett. 363 (2002) 123.
[10] H.T. Ng, J. Li, M.K. Smith, P. Nguyen, A. Cassell, J. Han, M. Meyyappan, Science 300 (2003) 1249.
[11] J.-J. Wu, S.-C. Liu, Adv. Mater. 14 (2002) 215.
[12] K. Ogata, K. Maejima, Sz. Fujita, Sg. Fujita, J. Crystal Growth 248 (2003) 25.
[13] Z.R. Dai, Z.W. Pan, Z.L. Wang, Adv. Funct. Mater. 13 (2003) 9.
[14] W.I. Park, G.-C. Yi, M. Kim, S.J. Pennycook, Adv. Mater. 15 (2003) 526.
[15] L. Guo, Y.L. Ji, H. Xu, P. Simon, Z. Wu, J. Am. Chem. Soc. 124 (2002) 14864.
[16] L. Vayssieres, K. Keis, S.-E. Lindquist, A. Hagfeldt, J. Phys. Chem. B 105 (2001) 3350.
[17] Z.R. Tian, J.A. Voigt, B. Mckenzie, M.J. Mcdermott, J. Liu, J. Am. Chem. Soc. 124 (2002) 12954.
[18] C.-H. Hung, W.-T. Whang, Mater. Chem. Phys. 82 (2003) 705.
[19] W.I. Park, G.-C. Yi, M. Kim, S.J. Pennycook, Adv. Mater. 14 (2002) 1841.
[20] S. Muthukumar, H. Sheng, J. Zhong, Z. Zhang, N.W. Emanaetoglu, Y. Lu, IEEE Trans. Nanotechnol. 2 (2003) 50.
[21] L. Vayssieres, Adv. Mater. 15 (2003) 464.
[22] K. Govender, D.S. Bolye, P. O'Brien, D. Binks, D. West, D. Coleman, Adv. Mater. 14 (2002) 1221.
[23] K. Vanheusden, W.L. Warren, C.H. Seager, D.R. Tallant, J.A. Voigt, B.E. Gnade, J. Appl. Phys. 79 (1996) 7983.
[24] C.-T. Hsieh, J.-M. Chen, H.-H. Lin, H.-C. Shih, Appl. Phys. Lett. 83 (2003) 3383.
[25] R.A. Laudise, E.D. Kolb, A.J. Caporaso, J. Am. Ceram. Soc. 47 (1964) 9.
[26] D.M. Bagnall, Y.F. Chen, Z. Zhu, T. Yao, M.Y. Shen, T. Goto, Appl. Phys. Lett. 73 (1998) 1038.
[27] Y.-K. Tseng, C.-J. Huang, H.-M. Cheng, I.-N. Lin, K.S. Liu, I.-C. Chen, Adv. Funct. Mater. 13 (2003) 811.
[28] C.X. Xu, X.W. Sun, Appl. Phys. Lett. 83 (2003) 3806.